Origami-adapted Clam Design for Wave Energy Conversion

Jingyi Yang[1]*, Zhong You[1], Shanshan Cheng[2], Xinyu Wang[2], Krishnendu Puzhukkil[2], Malcolm Cox[3], Rod Rainey[4], Siming Zheng[2], John Chaplin[4], Alistair Borthwick[2], Deborah Greaves[2]

Abstract—**The clam wave energy converter (WEC) is a floating device composed of two side plates connected by a hinge that closes and opens under interaction with wave crests and troughs. To convert the mechanical motions to electricity, either a linear power take-off (PTO) may be installed between the two side plates, or else the volume change may be used to pump air between chambers and across an air turbine PTO. The basic concept has been discussed since 1978 and featured as part of the UK Wave Energy research programme [1]. Several simplified clam models have been built since then and preliminary investigations were conducted at the COAST laboratory, University of Plymouth by Phillips [3] to understand wave-clam interactions. However, the simplified models were not enclosed and seawater became trapped in the device. To advance the investigation, we design the outer shell of the clam model to be properly enclosed and thus suitable for use in the marine environment. Inspired by origami, we construct the enclosed clam-type offshore device by connecting rigid panels and elastic membranes with rotational hinges. The rigid panels are modelled to rotate about the hinges without facet deformation whereas the membranes can be stretched. Strain on the elastic membrane is theoretically minimized for better structural integrity and minimal energy loss. By satisfying all the design requirements, the best geometric design is obtained through an optimization process. After that, a downscaled prototype is built to demonstrate that the strain incurred is negligible in response to the forces.**

Keywords—**floating clam, origami WEC, wave energy convertor, deployable structure, origami-adapted design, minimal strain.**

I. Introduction

OVER the last five decades, many different types of wave energy converters (WECs) have been proposed. A subset of these devices has garnered attention due to their ability to respond to wave motion through structural deformation. Table I summarizes the distinctive attributes of devices in this subset in terms of power take-off (PTO) mechanisms, modes of deformation, and typical dimensions.

TABLE I
EXAMPLES OF FLEXIBLE RESPONSIVE WEC CONCEPTS

Device	PTO				Deformation		Typical dimension		
	bellows-action with air turbine	bulge wave with Water turbine	distributed PTO, DEEC	direct drive	inelastic folding	elastic stretching	< 50m	50 – 100m	>100m
SQ1 [3-5]	X				X		X		
Fabriconda [6]		X			X				X
Anaconda [7]		X				X			X
S3 [8]			X			X			X
Bombora [9]					X	X			X
Floating clam [2,10]	X			X	X	X		X	

Sponsor and financial support acknowledgement: This work was supported in part by the EPSRC under grant EP/V040367/1

1 JY and ZY are with Department of Engineering Science, University of Oxford, Parks Road, Oxford, OX1 3PJ, UK (emails: *jyang.origami@gmail.com; zhong.you@eng.ox.ac.uk)

2 SC, XW, KP, SZ, AB, and DG are with School of Engineering, Computing and Mathematics, University of Plymouth, Drake Circus, Plymouth PL4 8AA, UK (emails: shanshan.cheng@plymouth.ac.uk; xinyu.wang-41@plymouth.ac.uk; krishnendu.puzhukkil@plymouth.ac.uk; siming.zheng@plymouth.ac.uk; Alistair.borthwick@plymouth.ac.uk; Deborah.greaves@plymouth.ac.uk)

3 MC is with Griffon Hoverwork Ltd., Hazel Road, Woolston, Southampton SO19 7GA, UK
(email: Malcolm.cox@griffonhoverwork.com)

4 RR and JC are with Faculty of Engineering and Physical Sciences, University of Southampton, Southampton SO16 7QF, UK (emails: R.Rainey@soton.ac.uk; j.r.chaplin@soton.ac.uk)

Digital Object Identifier: https://doi.org/10.36688/ewtec-2023-329

The present research investigates the floating clam type of WEC, due to its small geometry that enables cost reduction. Fig. 1 shows the first clam WEC, which was proposed and patented by Francis Farley [10]. As a floating device, the clam comprised two or more pressure vessels 1 and 10 interconnected by an air turbine 12 for PTO. The main vessel 1 had a V-shape composed of two rigid side plates connected by hinge 4 at the bottom and flexible airtight fabric 9 at the top. During operation, the clam is inflated and pressurized with air or other gas. Under wave action, the main vessel 1 oscillates both vertically in heave and in clam action whereby the clam walls rotate in and out at the hinge. The varying hydrostatic pressure exerted on the side plates 2 causes the main vessel to contract and expand, driving the gas into and out of the auxiliary vessel 10. Therefore, the energy carried by the waves is converted into the pneumatic energy of gas flowing through the air turbine connecting the vessels. The device is kept upright due to the ballast 5 underneath the main vessel.

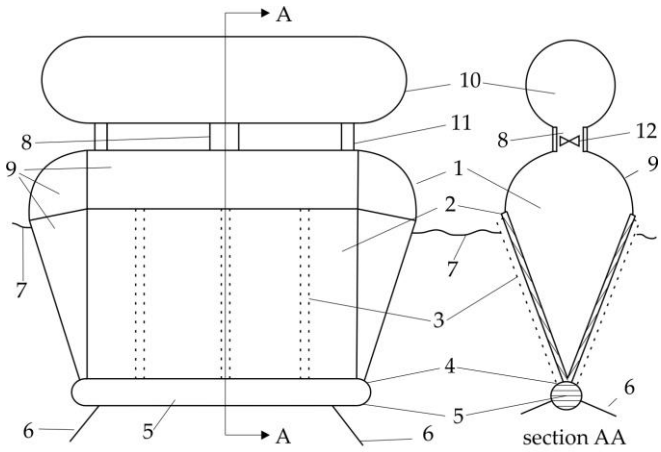

Fig. 1. The clam WEC proposed by Farley [2] (re-generated).

Moving on from Farley's concept, several simplified clam models have since been constructed, with the ballast 5 suspended below the main vessel 1 and with the rigid chamber 10 located elsewhere [2]. Preliminary investigations were conducted to understand the wave-structure interactions of the clam device at the COAST laboratory, University of Plymouth. These simplified models used a hydraulic ram as the PTO. They were not enclosed and hence seawater could be trapped in the device. To advance this concept, the present paper proposes an enclosed outer shell of the main vessel 1 which is suitable for use in the marine environment.

According to the bellows conjecture, no enclosed flexible polyhedral structure can change its volume without bending or stretching its facets [11, 12]. In other words, the clam WEC must be strained when it is in motion. In some PTO arrangements, e.g., the DEG, where energy is generated through stretching of the facets, the geometry of the clam-type WEC can be designed to maximize the strain in certain facets. In other PTO arrangements, e.g., the DFG, where energy is generated through bending, the geometry of the clam-type WEC can be designed such that the hinge length is maximized. In further PTO arrangements, such as mechanical linear actuators, air springs, and air turbines, where energy is not captured through bending or stretching of the material, a portion of the wave energy has to be consumed to deform the outer shell of the model and the remainder can be captured by the PTO. The design of the clam-type WEC in terms of such PTO arrangements aims to minimize the strain on its facets to maximize power extraction by the PTO; this is the focus of the present paper.

To achieve the objective outlined above, we can pursue two approaches in distributing strain within the structure during folding. The first approach involves evenly distributing the strain over the entire surface of the structure. By doing so, we ensure that no specific facets or regions of the structure bear excessive stress, thereby reducing the risk of failure or damage over time. Alternatively, we can design the folding patterns where only a small number of facets experience strain while the remainder of the structure remains strain-free. By concentrating the strain in specific areas, we can ensure that unaffected portions of the structure can withstand repeated folding and unfolding motions without significant degradation. This method allows for better control and management of strain, providing enhanced durability and reliability to the clam section.

In this paper, we will adopt the latter method and concentrate on the design of folding patterns where strain is limited to specific facets. Inspired by origami, we construct the enclosed clam-type WEC by connecting rigid panels and elastic membranes with rotational hinges. We will employ durable materials for the strained elastic membranes and enabling periodic inspection and replacement if necessary.

The paper is structured as follows. Section II proposes the design of the origami-adapted WEC, which involves a combination of rigid panels and elastic membranes through rotational hinges. The rigid panels are designed to rotate about the hinges without undergoing facet deformation, whereas the elastic membranes have the ability to stretch. It is essential to minimize strain within the elastic material in order to optimize structural integrity and minimize energy loss. Section III discusses the specific design requirements that need to be satisfied and outlines the steps involved in optimizing the geometric design of a clam section. To validate the effectiveness of the proposed design, Section IV presents a physical prototype to demonstrate and validate the performance and functionality of the design in a practical setting. Finally, Section V summarizes the key findings and contributions of the study.

II. THE ORIGAMI-ADAPTED MODEL

A. Clam motion

Fig. 2 presents a schematic illustration of the main vessel, in which two rigid plates, each of height h and width w, are hinged to form a V-shaped structure. To establish a reference frame for analysis, a Cartesian coordinate system O-xyz is positioned at the mid-point of the hinge as indicated in Fig. 2(a). The y-axis aligns with the rotational hinge and the z-axis is directed vertically upwards. The x-axis is determined by the right-hand rule. We introduce angle θ as a measure of the inclination between the O-yz plane and one of the side plates, as shown in Fig. 2(b). Notably, we can observe that the V-shaped clam exhibits symmetry with respect to the O-yz plane and the O-xz plane. The opening angle of the floating clam is 2θ.

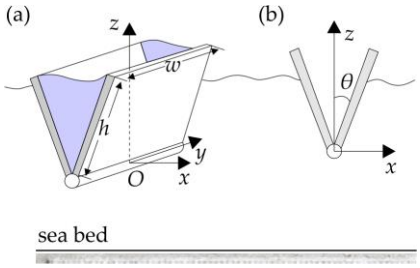

Fig. 2. (a) Isometric and (b) side view of the main vessel to illustrate the clam motion.

The motion of the main vessel can be decomposed into seven modes [13]. The first six modes arise from rigid body motion – modes 1 to 3 describe the translational motions along x, y, z axes (surge, sway and heave), whereas modes 4 to 6 describe the rotational motions about x, y, z axes (roll, pitch and yaw). Mode 7 is the first generalized mode, i.e., the clam mode, which is related to the energy captured by the PTO. The clam motion results from the clam mode, which is characterized by the changing opening angle 2θ of the floating clam.

B. The design variants

The main vessel of the clam device is a deployable structure comprising side plates and pleats. The placement of pleats is carefully designed to cover both the top surface and the side of the floating clam device. The primary objective of this design is to ensure that the pleats, serving as connections between the two side plates, form a closed body that facilitates the motion of the clam WEC while minimizing the strain exerted on the device.

Due to its inherent symmetry, the main vessel can be constructed by combining two identical origami-adapted clam sections placed side by side, wherein each section rotates through a dihedral angle θ as defined in Section II. Consequently, the task of designing the main vessel now turns into the design of a single clam section.

Fig. 3 presents the design configuration of a single clam section, showcasing two variants. Each variant consists of two side surfaces, namely AEPQ and DHPQ, which are connected by top pleats ABFE and DBFH, side pleats AQC and DQC, and triangles ABC, BCD, EFG and FGH (with vertex G not visible in the figure). Notably, the small triangles located at the corners (ABC, BCD, EFG, and FGH) are constructed using elastic membranes, whereas the remaining facets are represented as rigid plates. The connections between panels or sheets can be established using rotational hinges, such as piano hinges or door hinges, which are specifically selected for their simplicity and durability. These hinges allow for the rotation of panels or sheets, facilitating the change of angle θ of each clam section.

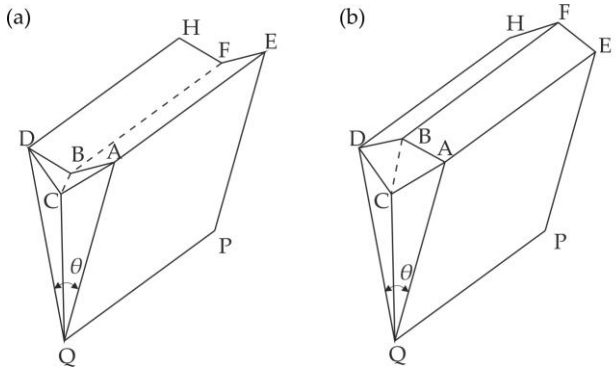

Fig. 3. Two design variants of a clam section with top pleats contracting inwards in (a) and bulging outwards in (b).

In Fig. 3, the solid lines represent mountain folds, whereas the dotted lines represent valley folds. It is important to note that for valley folds, the rotational hinges are placed on the outer surface, whereas for mountain folds, they are placed on the inner surface. Specifically, the top pleats form a valley fold in Fig. 3(a), whereas they form a mountain fold in Fig. 3(b). Consequently, as the angle θ decreases, the top pleats contract inward in Fig. 3(a), whereas they bulge outward in Fig. 3(b). Similarly, the side pleats also exhibit two design variants: they can either bulge outward as the angle θ decreases, as illustrated in Fig. 3, or contract inward. Therefore, when considering combinations of side pleats and top pleats, a total of four design variants emerges. The configuration that demonstrates the minimum strain during its motion will be determined through an optimization process, which will be introduced in section III and subsequently adopted for the physical model construction.

III. OPTIMIZATION

A. Local coordinate system

A local coordinate system O-xyz is established to more clearly describe the motion of a clam section in Fig. 4. Its origin O is positioned at the mid-point of the rotational joint where the two side surfaces intersect. The y-axis is aligned with the rotational hinge, whereas the z-axis is

oriented upwards. This arrangement of the coordinate system ensures that both the *O-yz* plane and the *O-xz* plane function as planes of symmetry for the clam section. Throughout the contraction and expansion processes, design considerations are implemented to maintain the symmetrical properties of the clam section with respect to the *O-yz* and *O-xz* planes.

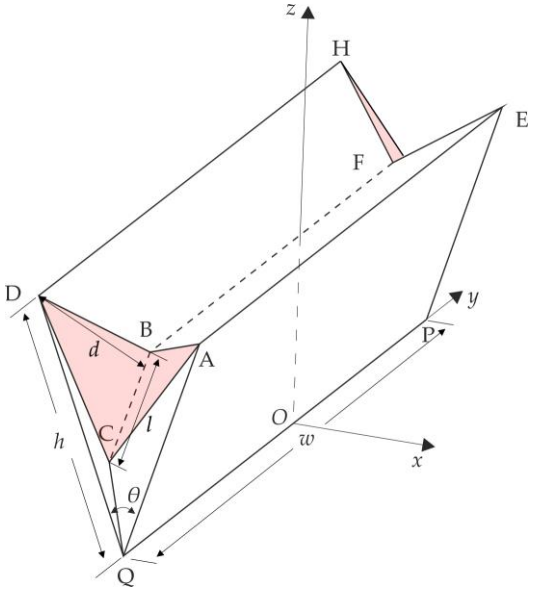

Fig. 4. A clam section with plane symmetry.

B. Design parameters

Certain parameters are predetermined based on hydrostatic requirements, including the dimensions of the side plates, represented by the width (w) and height (h), as well as the equilibrium opening angle (θ_{eq}) of a clam section. Considering hydrodynamic efficiency and the stability of the floating clam, the width (w) of the side plate is twice the height (h) in this example. The two side plates oscillate about their equilibrium position θ_{eq}, ranging from a minimum angle of 0° to a maximum opening angle of $\theta_{max} = 2\theta_{eq}$. Subsequently, the remaining dimensions are determined in relation to these three predefined parameters. One approach is to set the sector angles ∠AQC and ∠DQC to half the maximum opening angle θ_{max}. By applying trigonometry, the distance between BF and DH, denoted as a, can be obtained as $a = h \cdot \sin(\angle AQC)$. In this way, the clam section can achieve its maximum opening angle when the dihedral angle between side pleats AQC and DQC reaches 180°. Additionally, the dihedral angle between top pleats ABFE and DBFH also reaches 180°.

C. Objective function

The design parameters are correlated through trigonometry, enabling calculation of the remaining parameters upon determining the side lengths QC and BF. However, due to space constraints, we do not elaborate further on the calculations. Our objective is to optimize the lengths of QC and BF for minimum strain in the elastic membranes highlighted in Fig. 4.

When the clam section is contracted or opened, the elastic membranes stretch or slacken, whereas the rigid plates undergo rigid body motion about the rotational hinges. To analyse the behaviour of the system, it is necessary to calculate the average strain stored in the elastic facets throughout its full range of motion.

In the context of the triangular facet BCD, the planar strain ε is defined as the root-mean-square of the tensile strain components in two orthogonal directions on the surfaces. As shown in Fig. 4, the length BC of the triangular facet is denoted by the variable l, and the shortest distance from vertex D to edge BC is represented by d. Therefore, the strain of a surface can be calculated from

$$\varepsilon = \frac{1}{2}\sqrt{\left[\max\left\{(l-l_0),0\right\}/l_0\right]^2+\left[\max\left\{(d-d_0),0\right\}/d_0\right]^2} \quad (1)$$

where l_0 and d_0 represent the original dimensions of the elastic triangles BCD and ABC, and l and d represent the stretched lengths. It is worth noting that the operation max{} truncates any negative values of $(l - l_0)$ given that the membrane would enter a slack state if it experiences compression.

Throughout the full range of motion of the clam section, the average strain on the elastic membrane is given by

$$\bar{\varepsilon} = \frac{\int_0^{\theta_{\max}} \varepsilon d\theta}{\theta_{\max}} \quad (2)$$

where ε denotes the instantaneous strain of the elastic membrane when the clam section has an opening angle θ.

Therefore, we minimize $\bar{\varepsilon}$ in (2) subject to the change of QC and BF. The objective function is formulated as

$$\min f(\text{QC, BF}) = \frac{\int_0^{\theta_{\max}} \varepsilon d\theta}{\theta_{\max}} \quad (3)$$

In addition, to ensure structural integrity of the clam section, constraints are imposed on the lengths. Specifically, the lengths are allowed to vary within the upper and lower bounds as specified by the user. In our case, the limits are

$$\begin{cases} h/5 \le \text{QC} \le h, \\ 4w/5 \le \text{BF} \le w \end{cases} \quad (4)$$

The optimization process starts with an initial guess of the lengths, e.g., QC = h/5 and BF = 4w/5. The process advances until a local minimum is found using the Matlab *fmincon* function [14] via an interior-reflective Newton approach [15].

IV. RESULTS AND DISCUSSION

A. The optimized design

Given the pre-defined aspect ratio of the side plate of a clam section, $w = 2h$ when considering both the structural stability and hydrodynamic efficiency of the device. By setting the maximum opening angle of a clam section to 40° or 60°, we can calculate the angles ∠AQC and ∠EPG, which are half of the maximum opening angles in each case. To obtain the optimized parameters, we perform a search for the local minimum. Subsequently, the remaining geometric parameters are determined using trigonometric calculations. Table II presents the dimensions of the clam section for each case.

TABLE II
DIMENSIONS FOR THE MINIMAL STRAIN DESIGN

	$0 \le \theta \le 40°$	$0 \le \theta \le 60°$
∠AQC = ∠AQD = ∠EPF = ∠HPF	22.5°	30°
∠BAC = ∠BDC = ∠FEG = ∠FHG	44°	28.09°
BF	80% w	90% w
AB = BD = EF = HF	21.57% w	26.48% w
QC = PG	42.02% h	40% h
AC = CD = EG = HG	63.26% h	68.35% h

In addition, the maximum planar strains on the elastic triangular membrane during the full range of motion are set to 1.27% and 1.78% to achieve the opening angle of 40° and 60°, respectively. Fig. 5 illustrates a fully expanded and a fully contracted clam section with a maximum opening angle of 40°, wherein the elastic membranes are highlighted in red.

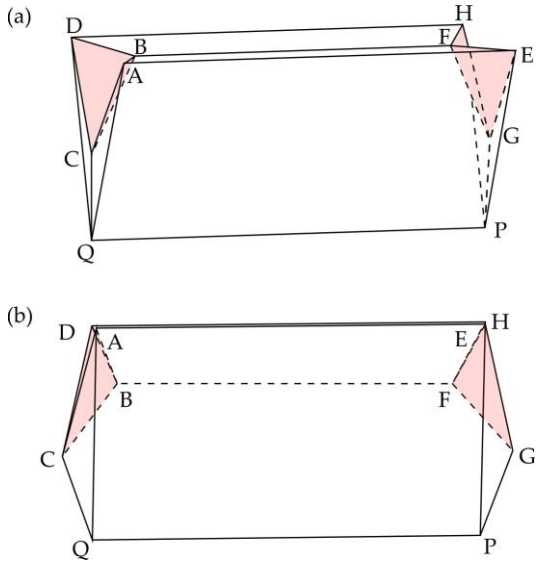

Fig. 5. A clam section in (a) fully expanded configuration and (b) fully closed configuration. Elastic regions are highlighted in red.

A physical prototype has been constructed to demonstrate the minimal strain experienced during the contraction and expansion motions of the clam section. The strain level is so insignificant that the physical model can successfully contract and expand, even with all facets constructed using rigid plywood, as shown in Fig. 6.

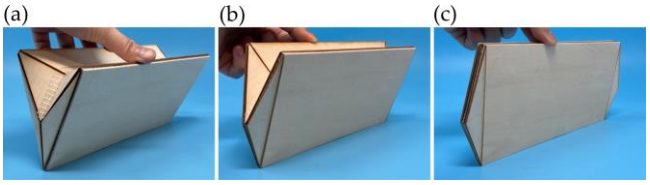

Fig. 6. A physical prototype made of plywood in its (a) fully expanded state, (b) equilibrium state, and (c) fully contracted state.

To illustrate the functionality of the prototype, a small force was manually applied to separate the two rectangular side plates in Fig. 6(a), bringing it to its fully expanded configuration. Conversely, a small force was applied to pinch the side plates together, achieving the fully closed state as depicted in Fig. 6(c). In Fig. 6(b), no external force was applied, and the model is shown in its equilibrium position with the hand being used solely to maintain the clam model in an upright position.

B. The design of the floating clam

Fig. 7 serves as an illustrative representation of the design of the floating clam in its expanded configuration. Fig. 7(a) provides an isometric view alongside a cross-sectional view denoted as BB. Fig. 7(b) presents the top, front, and side views of the vessel. Owing to its inherent symmetry, the main vessel comprises two identical clam sections (designated as 100) with each exhibiting an opening angle θ, according to the definition given in Section II. These clam sections are affixed side by side to a central rigid frame (labelled as 102). Furthermore, the central rigid frame is connected to the ballast (represented as 107) at the bottom of the main vessel through support bars (106).

The two clam sections are attached to a side face (identified as 101), which can be constructed from robust materials such as carbon fibre-reinforced composites (CFRP) or plywood. The connection between the rigid side panel and the central frame involves utilization of two identical trapezoidal-shaped sheets (labelled as 103) as top pleats, as well as four abstruse triangular sheets (designated as 104) on the two sides. As for the side panels, these sheets can be manufactured from durable materials like CFRP or plywood. Moreover, an additional four identical triangular sheets (referred to as 105) connect sheets 104 with sheets 103 and can be fabricated from elastic reinforced rubber. This rubber material allows for greater facet deformation under strain and is specifically designed to experience tension while remaining slack under compression.

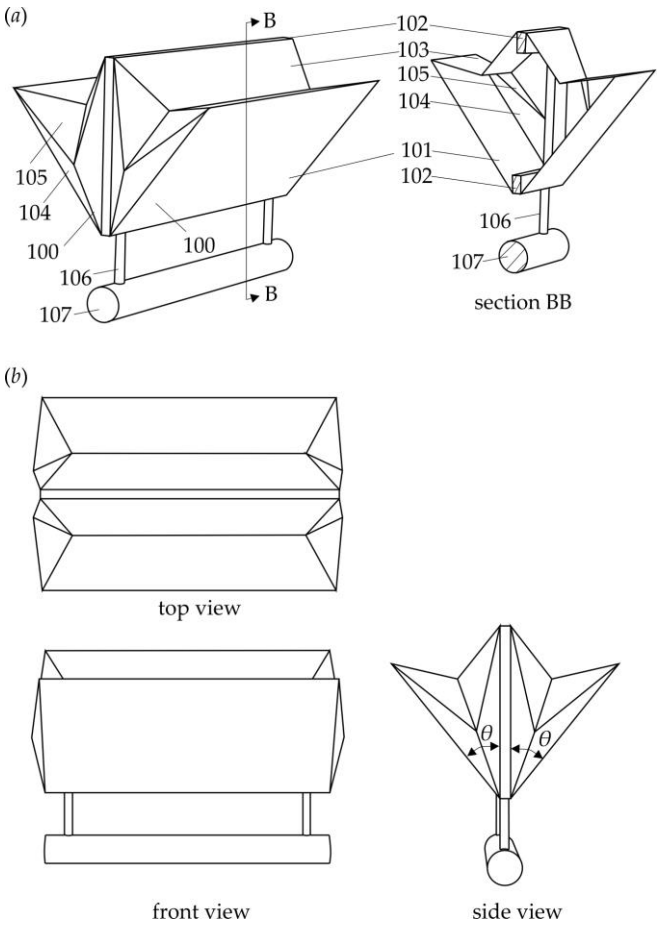

Fig. 7. Main vessel design in (a) isometric and (b) plan views.

C. *Interactions with sea wave*

In the presence of wave conditions and coupling between the clam mode and heave mode, the main vessel of the device interacts with waves, causing fluctuations in the hydrostatic pressure acting on the side plates due to the heaving motion. In the initial state, the floating clam is at rest in still water, and each clam section has an equilibrium opening angle θ_{eq}. During wave crests, the hydrostatic pressure surpasses the internal pressure provided by the PTO system, causing the main vessel to contract, and θ to decrease. Conversely, during wave troughs, the hydrostatic pressure falls below the internal pressure generated by the PTO system, causing the main vessel to expand and θ to increase. Consequently, each clam section compresses and expands as the side plates interact with wave crests and troughs, enabling the PTO system to effectively capture wave energy.

In the presence of adverse environmental conditions, such as storms and extreme waves, the device should be able to adopt a survivability state. In this state, the clam model can be closed and the angle θ approaches zero, causing the device to sink underwater. The geometry of the clam section is designed such that small strain is induced in the elastic sheets when in the fully folded state. This specific configuration ensures the device exhibits resilience to adverse conditions without compromising the structural integrity of the elastic sheets.

V. CONCLUSION

This paper has presented an origami-adapted design for the outer shell of a clam wave energy converter, focusing on achieving optimal performance in the marine environment. The design ensures a fully enclosed body, suitable for withstanding extreme wave conditions. Through optimization of the geometry of the clam section, strain experienced during expansion and contraction motions has been minimized. This optimization strategy aims to prolong the fatigue life of the structure while maximizing the energy captured by PTO. To demonstrate the effectiveness of the design, a downscaled physical prototype was constructed from rigid plywood. The prototype highlights the minimal strain experienced by the clam section during its motion.

In future work, our research will concentrate on characterizing the force required to cause the model to deviate from its equilibrium position. This characterization will provide insight into the structural behaviour of the clam section.

REFERENCES

[1] Peatfield, A. M., Duckers, L. J., Lockftt, F. P., Loughridge, B. W., West, M. J., & White, P. R. S. (1984). The SEA-Clam wave energy converter. In *Energy Developments: New Forms, Renewables, Conservation* (pp. 137-142). Pergamon.

[2] Phillips, J. W. (2017). *Mathematical and Physical Modelling of a Floating Clam-type Wave Energy Converter* (Doctoral dissertation, University of Plymouth).

[3] Kurniawan A, Chaplin J, Greaves D, Hann M., and Farley, F. (2017). Wave energy absorption by a floating air bag, *Journal of Fluid Mechanics* 812:294-320.

[4] Kurniawan A, Greaves D, Chaplin J. (2014). Wave energy devices with compressible volumes. *Proc. R. Soc. A* 470: 20140559.

[5] Kurniawan, A., Chaplin, J.R, Hann, M.R, Greaves, D.M, Farley, F.J.M. (2017) Wave energy absorption by a submerged air bag connected to a rigid float, *Proc. R. Soc. A*, 10.1098.

[6] Hann, M. R. (2013). *A numerical and experimental study of a multi-cell fabric distensible wave energy converter* (Doctoral dissertation, University of Southampton).

[7] Farley F., Rainey R. & Chaplin J (2012) Rubber tubes in the sea. *Phil. Trans. R. Soc. A*, 370, 381-402.

[8] Babarit, A., Singh, J., Mélis, C., Wattez, A., & Jean, P. (2017). A linear numerical model for analysing the hydroelastic response of a flexible electroactive wave energy converter. *Journal of Fluids and Structures*, 74, 356-384.

[9] Bombora (2019), https://www.bomborawave.com/

[10] Farley, F. J. M. (2012). Free floating bellows wave energy converter. *UK Patent GB2488185*.

[11] Connelly, R. (1977). A counterexample to the rigidity conjecture for polyhedra. *Publications Mathématiques de l'IHÉS*, 47, 333-338.

[12] Connelly, R., Sabitov, I., & Walz, A. (1997). The bellows conjecture. *Beitr. Algebra Geom*, *38*(1), 1-10.

[13] Zheng, S., Phillips, J. W., Hann, M., & Greaves, D. (2023). Mathematical modelling of a floating Clam-type wave energy converter. *Renewable Energy*, *210*, 280-294.

[14] Matlab optimization toolbox - fmincon, mathworks, R2019b, (2020), [Online]. Available: https://uk.mathworks.com/help/optim/ug/fmincon.html# References. (Accessed 15 February 2023).

[15] T.F. Coleman, Y. Li (1994). On the convergence of interior-reflective Newton methods for nonlinear minimization subject to bounds, *Math. Program*. 67 189–224.